ISSN 1068-3755, Surface Engineering and Applied Electrochemistry, 2015, Vol. 51, No. 5, pp. 434–439. © Allerton Press, Inc., 2015.

Microwave-Hydrothermal Synthesis of Nb-Doped $BaTiO_3$ Nanoparticles under Various Conditions[1]

A. Khanfekr*, M. Tamizifar, and R. Naghizadeh

Department of Metallurgical and Materials Engineering, Iran University of Science and Technology (IUST), Narmak, Tehran, Iran

**e-mail: khanfekr@iust.ac.ir*

Received August 13, 2014; in final form, November 24, 2014

Abstract—Tetragonal $BaTiO_3$ powders were synthesized by the microwave-hydrothermal (MH) method. The effects of the reaction time and temperature on the MH synthesis were investigated. Typical experiments were performed with a solid state reaction for the system $BaTiO_3$ + Nb_2O_3 at a high temperature. In the MH method, at a shorter time and lower temperature, the rate of the formation of tetragonal $BaTiO_3$ and of the growth of particles went down substantially. The microwave heating can be very fast and uniform through a self-heating process that results from the direct absorption of the microwave energy in the reaction mixture. The synthesis of Nb-doped $BaTiO_3$ has been investigated under MH conditions in the temperature range of 120–180°C for 1–3 hours using $C_{16}H_{36}O_4Ti$, $BaH_2O_2 \cdot 8H_2O$, and $NbCl_5$ as Ba, Ti and Nb sources, respectively. In the phase evolution studies, the X-ray diffraction measurements and Raman spectroscopy were employed. The Transmission Electron Microscope and the Field Emission Scanning Electron Microscopy images were taken for the detailed analysis of the grain size, surface, and morphology. The MH method was applied for the synthesis of Nb-doped $BaTiO_3$ via provided advantages of the fast crystallization and decreased crystallite size. The nucleation rate should have been high because of a high heating rate in microwave heating processes.

Keywords: ceramics, chemical synthesis, microwave-hydrothermal synthesis, crystal structure, perovskites

DOI: 10.3103/S1068375515050063

INTRODUCTION

Perovskite-type oxides have the general formula of ABO_3 in which A is a rare earth or alkaline earth metal and B is a transition metal. Applications of this group of materials in electrochemistry [1, 2], oxygen separation membranes [3], chemical sensors for the detection of humidity [4], alcohol [5], gases such as oxygen [6] and hydrocarbon [7], and of nitric oxide [8] for over 30 years are the basis for understanding their mixed conductivity by both ion and electron migrations and their high nonstoichiometric composition. Since there is a strong dependence of ferroelectric properties on the grain size and compositional aspects, the microstructural control has become very important [9]. $BaTiO_3$-based positive temperature co-efficient (PTC) thermistors are widely used as over-current protectors, motor starters for refrigerators and air conditioners, temperature sensors, and so on [10–14]. The hydro-thermal method is attractive for synthesizing $BaTiO_3$ powder because the combined effects of the solvent, temperature, and pressure on the ionic reaction equilibrium can stabilize desirable products while inhibiting formation of undesirable compounds. Hydro-thermal synthesis also makes it possible to prepare $BaTiO_3$ powder in a single processing step and does not require elaborate apparatuses or expensive reagents However, just like in most convectional hydro-thermal processes, $BaTiO_3$ powders prepared by the microwave-hydrothermal (MH) synthesis at temperatures below 200°C were cubic or pseudo cubic, though the tetragonal structure is thermodynamic, stable at room temperature. To convert hydrothermal $BaTiO_3$ from the cubic to tetragonal shape, heating at temperatures over 1000°C is required, which always leads to the grain growth and particle aggregation. Therefore, a direct generation of tetragonal $BaTiO_3$ through the hydrothermal process is of a considerable interest, both in science and in industry [13–15].

It has been reported [15, 16] that the nanostructural and dielectric features of nano-sized Nb-doped $BaTiO_3$ powders vary sensitively with their size and preparation conditions. To the best of our knowledge, there are few reports on the doped $BaTiO_3$ metal-semiconductor transition on Nb doping, in particular. Sintered bulk ceramics of Nb-doped $BaTiO_3$ show the semiconducting behavior when doped with a small amount of Nb, but when Nb concentration exceeds 0.4–0.5 mol %, the specimens revert to the insulator state. The main reason for the increase of resistivity when the donor concentration exceeds a certain value

[1] The article is published in the original.

is the fact that the compensation mechanism changes from one that mainly involves electrons to one that primarily involves cation vacancies [15–18]. In the present paper, we analyze the effect of incorporating different amounts of Nb on the microstructural development of $BaTiO_3$. A particular emphasis is placed in the morphology and composition of secondary phases.

Compared to the traditional solid-state reaction and other wet-chemical routes (including sol-gel processing, oxalate route, and homogeneous precipitation), the hydrothermal method is low-cost and convenient to prepare $BaTiO_3$ nanoparticles without a following high temperature calcination process [16–21]. In order to produce powders of a desired size and shape, several researchers investigated a variety of hydrothermal conditions, such as the pH value, Ba/Ti ratio, reaction temperature as well as various precursors [21–25]. Though many efforts have been pulled to prepare $BaTiO_3$ particles, still there is insufficient knowledge about the effects of doping and solvent type on the size and shape under hydrothermal conditions. A number of authors [21–25] have synthesized $BaTiO_3$ by the MH method at T below 200°C but the MH processing of Nb-doped $BaTiO_3$ has not been reported so far with other authors. We succeeded in our initial efforts to synthesis of Nb doped $BaTiO_3$ in the temperature of 150°C for only 2 hours [26]. Therefore in this work, we have investigated the effect of incorporating Nb on the properties of $BaTiO_3$ via the MH conditions in the temperature range of 120–180°C for 1–3 hours.

EXPERIMENTAL

The MH reactions were performed to synthezise Nb-doped $BaTiO_3$. For more details, please, refer to our earlier manuscript [26]. The system was heated in the temperature range of 120–180°C for 1–3 hours. The obtained powders were characterized by the X-ray diffraction (XRD), with the CuK_α radiation in the 2θ range from 20° to 60° and Raman spectroscopy (spectral range 80–3500 cm^{-1}). Micro-structural characterization was performed by the field emission scanning electron microscopy (FE-SEM) and transmission electron microscopy (TEM).

RESULTS AND DISCUSSION

Figure 1 shows the XRD patterns for the MH Nb-doped $BaTiO_3$ powders prepared in the temperature range of 120–180°C for 1–3 hours. From the XRD patterns it can be considered that the sample prepared at 120°C for 1 h (MH-120-1) forms a pattern similar to an amorphous product, but when the time and temperature rise, the $BaTiO_3$ powder becomes a structurally uniform crystalline with high crystallinity. Except the sample prepared at 120°C for 2 h (MH-120-2), the nanoparticles were pure perovskite Nb-$BaTiO_3$, without some intermediate carbonate phase that was observed at 2θ 28° and 34° in the sample MH-120-2 [16]. The presence of $BaCO_3$ can be accounted for either by an incomplete reaction or by the presence of carbonate in the Ba alkali source, or by the reaction of CO_2 in air [14].

It is clearly seen that with the enhancement of time and temperature, the maximum of the peak shifts towards higher 2θ values and the intensity of the peaks grows. According to the investigations of some researchers [28, 29], the shift of peaks can be related to the displacements of barium. In the tetragonal phase, the optimization of the crystal geometry of $BaTiO_3$ after doping with Nb is attained by the impurity-outward displacements of barium. The movements are mainly in the *ab* plane while the motion along the *c* axis is practically negligible. In the sample synthesis at the highest time and temperature, we have the highest intensity.

When the size of $BaTiO_3$ powders is below 1 μm, the full-width at half-maximum (FWHM) of the corresponding (110) XRD peaks becomes larger and such broadening leads to the overlapping of two peaks located close to each other [14, 23, 27]. The structural changes associated with the phase transition usually have a large effect on the Raman spectrum. The XRD studies produce data that are consistent with an increasingly cubic structure at smaller particle sizes, not distinguishing between an average and a local structure. Thus, the XRD patterns reveal the characteristics of cubic $BaTiO_3$ without certain peak splitting while the Raman results have supported the existence of a tetragonal symmetry at small dimensions, even though it was not discernible by XRD. The Raman spectra for the obtained Nb-$BaTiO_3$ ceramic powder samples are presented in Fig. 2. The peaks at 185, 305, 518 and 715 cm^{-1} are characteristics of the tetragonal $BaTiO_3$. The peaks at 191 and 392 cm^{-1} are assigned to TiO_2 [30–33].

The dependence of the degree of the tetragonal fraction on the particle size has been extensively investigated for $BaTiO_3$ [23, 30]. A variety of explanatory models were proposed and researchers reported that the tetragonal distortion decreased when the particle size was below 1 μm [23, 24]. Thus, a reasonable explanation for a larger tetragonality in the sample synthesized at 180°C is the fact that the particles grow faster under MH conditions and at higher temperatures.

The FE-SEM images of Nb-$BaTiO_3$ powders prepared at 150 and 180°C for 2 h are shown in Figs. 3 and 4, respectively. It is evident that the powder prepared at 150°C consists of ultrafine, well dispersed uniform particles with the average size of 45 nm, the particle size being distributed from 40 to 50 nm. Whereas for the powders synthesized at 180°C, the average particle size increases substantially to the average size of

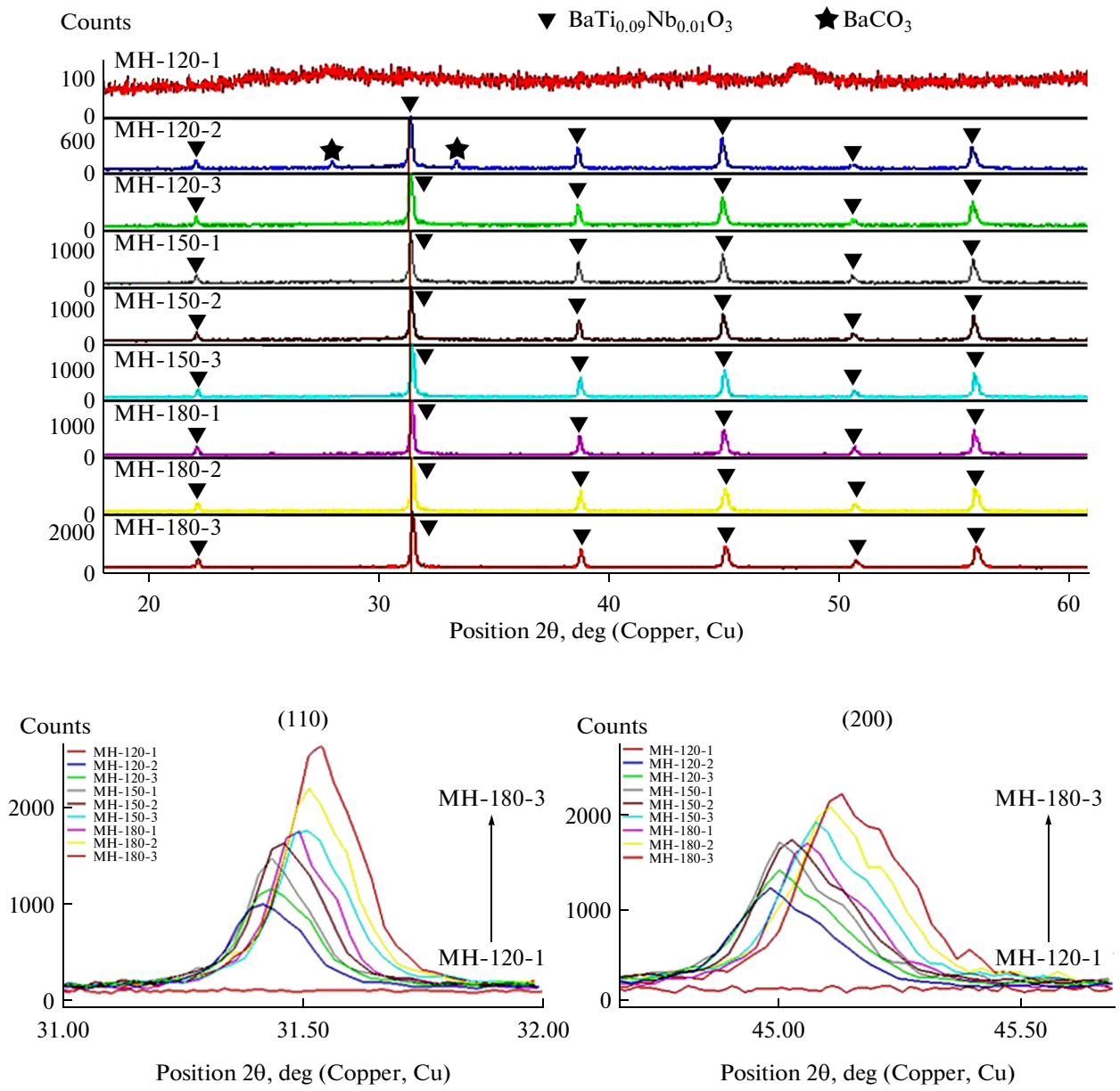

Fig. 1. XRD patterns of Nb-$BaTiO_3$ nanoparticles at different time and temperature: (Up) Zoom in (110) and (200) planes (Down).

90 nm, with the particle size distribution being from 70 to 110 nm.

In the MH process, the microwave radiation can be absorbed by $BaTiO_3$ particles and smaller $BaTiO_3$ particles will dissolve more quickly. According to the dissolution/recrystallization mechanism, this will lead to larger particles growing faster with time and temperature [23, 32, 33].

The MH synthesis leads to the homogeneous nucleation of a large number of tiny stable Nb-BT particles, which further grow uniformly; the primary Nb-BT particles form agglomerates [24, 28].

The crystallite size of the particles was calculated with the XRD using the Scherrer equation as in [35]:

$$D_v = \frac{K\lambda}{B_{size}\cos\theta}, \quad (1)$$

where D_v is the crystallite size, K is a constant whose value is 0.9, λ is the X-ray wavelength; the width of the peak, B_{size}, was determined as the full width at half-maximum. The crystallite size was 52 and 95 nm for the Nb-$BaTiO_3$ powder prepared at 150 and 180°C for 2 hours, respectively. These results are in good agreement with the FE-SEM data, too.

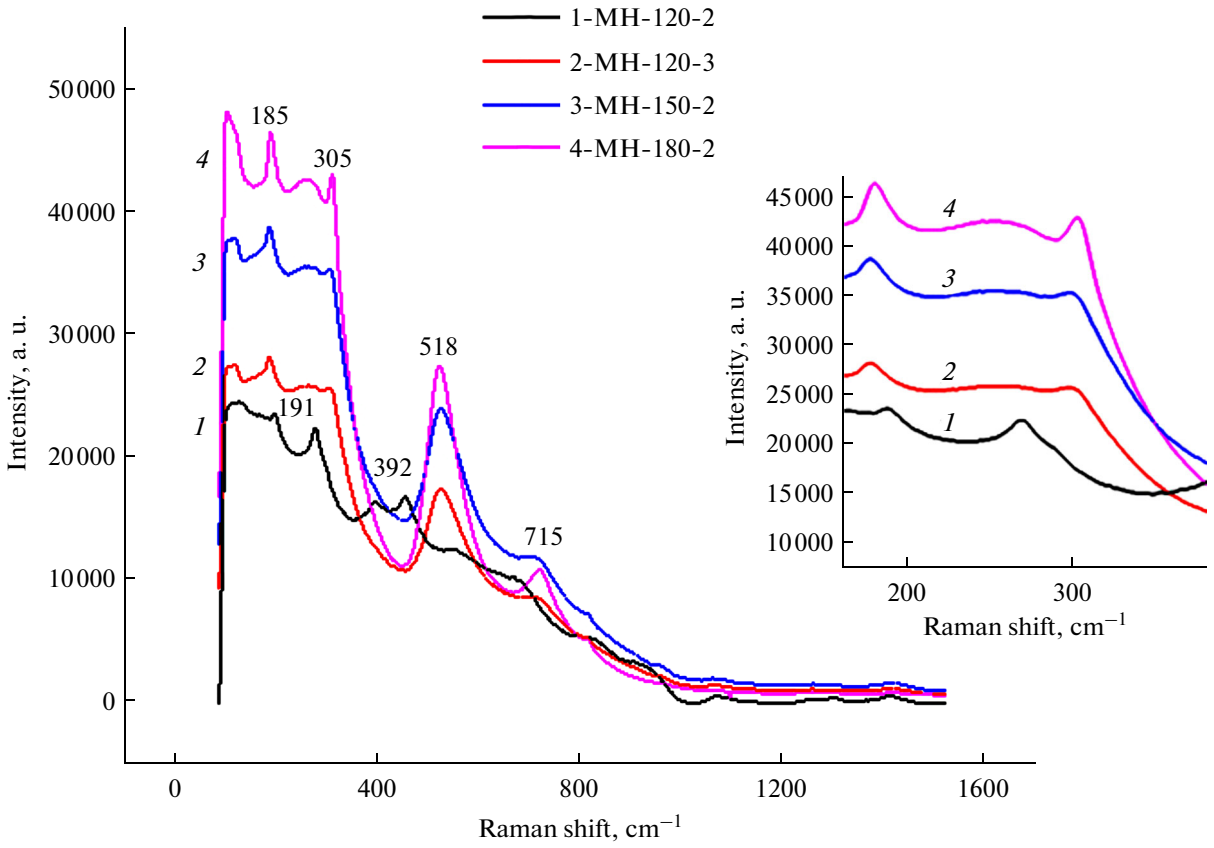

Fig. 2. Raman spectra of hydrothermal nanosized Nb-$BaTiO_3$ powders.

The TEM images taken to estimate the size of the particles and the morphology of the particles for powders prepared at 150 and 180°C for 1 h are shown in Figs. 5 and 6, respectively. The decreased crystal size in MH-150-2 might be related to a high heating rate in MH processes. At the microwave frequency of 2.45 GHz, the changes of plus/minus in the waveguide occur 2450 million times in 1 s. Depending on the characteristics of the dielectric, it tends to modify the alternating electric field through structural changes. When a water sample is placed in a reactor and subjected to an alternating electric field, the electric deviation (electric dipole) of the water molecule tends to follow the alternating electric field. However, since water consists of clusters of water molecules through hydrogen bonding, not all can follow the alternating electric field. The result is the dielectric heating of water by the irradiating microwaves. Moreover, as for

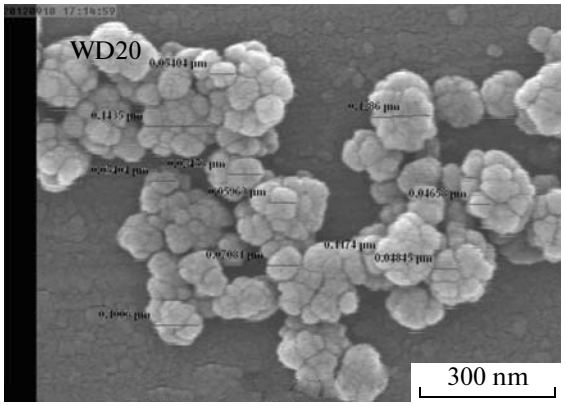

Fig. 3. Nb-$BaTiO_3$ powder prepared at 150°C for 2 h.

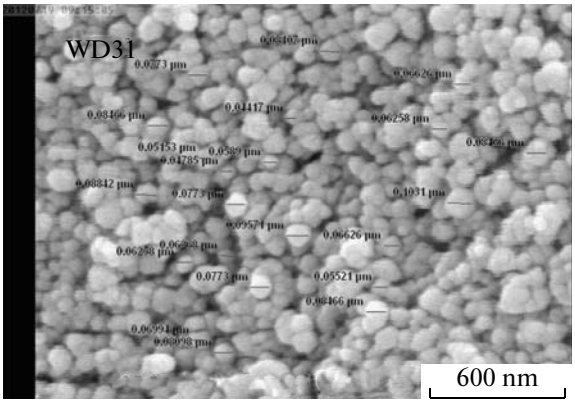

Fig. 4. Nb-$BaTiO_3$ powder prepared at 180°C for 2 h.

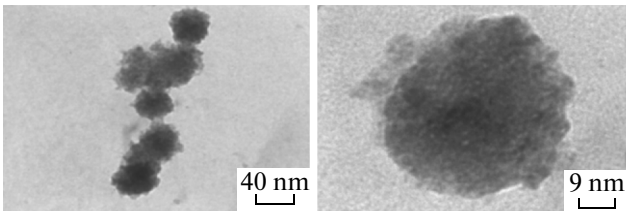

Fig. 5. Nb-$BaTiO_3$ powders prepared at 150°C for 1 h.

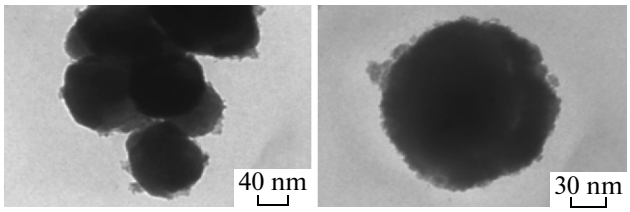

Fig. 6. Nb-$BaTiO_3$ powders prepared at 180°C for 1 h.

the case of ions in solution, the Joule heating takes place by space-charge polarization. When microwave heating, an electrolyte-water solution dielectric heating, and the Joule heating occur simultaneously, compared with pure water, then exothermic efficiency becomes remarkably high. Accordingly, dielectric heating by orientation polarization of water and resistance heating by the Joule process are enhanced in electrolyte—water media. This rapid homogeneous heating, not possible by convectional heating, provides a uniform nucleation [36].

CONCLUSIONS

The present investigation shows that nanosized particles of Nb-$BaTiO_3$ powder can be crystallized via a rapid and cost-effective MH process without the temperature gradient and uneven nucleation and growth of particles of various sizes. The MH can be very fast and uniform through a self-heating process that arises from the direct absorption of the microwave energy in the reaction mixture. When microwave heating an electrolyte–water solution dielectric heating and the Joule heating occur simultaneously compared with pure water, and thus exothermic efficiency becomes remarkably high. Accordingly, dielectric heating by orientation polarization of water and resistance heating by the Joule process are enhanced in electrolyte—water media. This rapid homogeneous heating, not possible by convectional heating, provides a uniform nucleation. Because of a homogeneous nucleation, uniformly-sized particles can be prepared. But according to the dissolution/recrystallization mechanism, both the extent of tetragonality and the particle size increase quickly with time and temperature. When the reaction temperature goes down, the formation of the tetragonal structure and growth of particles are slowed down substantially, showing a critical effect of the reaction temperature on the MH processing of tetragonal $BaTiO_3$.

REFERENCES

1. Kharton, V.V., Yaremchenko, A.A., and Naumovich, E.N., Research on the electrochemistry of oxygen ion conductors in the Former Soviet Union, II: Perovskite-related oxides, *J. Solid State Electrochem.*, 1999, vol. 3, no. 6, pp. 303–326.
2. Bi, Z., Cheng, M., Dong, Y., Wu, H., She, Y., and Yi, B., Electrochemical evaluation of $La_{0.6}Sr_{0.4}CoO_3$–$La_{0.45}Ce_{0.55}O_2$ composite cathodes for anode-supported $La_{0.45}Ce_{0.55}O_2$–$La_{0.9}Sr_{0.1}Ga_{0.8}Mg_{0.2}O_{2.85}$ bilayer electrolyte solid oxide fuel cells, *Solid State Ionics*, 2005, vol. 176, nos. 7–8, pp. 655–661.
3. Takamura, H., Enomoto, K., Aizumi, Y., Kamegawa, A., and Okada, M., Preparation and oxygen permeability of Pr–Al-based perovskite-type oxides, *Solid State Ionics*, 2004, vol. 175, nos. 1–4, pp. 379–382.
4. Holc, J., Slunečko, J., and Hrovat, M., Temperature characteristics of electrical properties of (Ba,Sr)TiO_3 thick film humidity sensors, *Sensors Actuators, Ser. B*, 1995, vol. 26, no. 1–3, pp. 99–102.
5. Kong, L.-B. and Shen, Y.-S., Gas-sensing property and mechanism of $Ca_xLa_{1-x}FeO_3$ ceramics, *Sensors Actuators, Ser. B*, 1996, vol. 30, no. 3, pp. 217–221.
6. Lukaszewicz, J.P., Miura, N., and Yamazoe, N., A LaF_3-based oxygen sensor with perovskite-type oxide electrode operative at room temperature, *Sensors Actuators, Ser. B*, 1990, vol. 1, nos. 1–6, pp. 195–198.
7. Brosha, E.L., Mukundan, R., Brown, D.R., Garzon, F.H., Visser, J.H., Zanini, M., Zhou, Z., and Logothetis, E.M., CO/HC sensors based on thin films of $LaCoO_3$ and $La_{0.8}Sr_{0.2}CoO_{3-\delta}$ metal oxides, *Sensors Actuators, Ser. B*, 2000, vol. 69, nos. 1–2, pp. 171–182.
8. Traversa, E., Matsushima, S., Okada, G., Sadaoka, Y., and Sakai, Y., Watanabe: NO_2 sensitive $LaFe_3$ thin films prepared by r.f. sputtering, *Sensors Actuators, Ser. B*, 1995, vol. 25, no. 1, pp. 661–664.
9. Vijatović, M.M., Bobić, J.D., and Stojanović, B.D., History and challenges of barium titanate, Part I, *Sci. Sintering*, 2008, vol. 40, pp. 155–165.
10. Kim, H.T. and Han, Y.H., Sintering of nanocrystalline $BaTiO_3$, *Ceram. Int.*, 2004, vol. 30, no. 7, pp. 1719–1723.
11. Bomlai, P., Effects of surrounding powder in sintering process on the properties of Sb and Mn-doped barium strontium titanate PTCR ceramics, *Songklanakarin J. Sci. Technol.*, 2006, vol. 28, no. 3, pp. 669–675.
12. Yoo, H.-I. and Song, Ch.-R., Thermoelectricity of $BaTiO_{3+\delta}$, *J. Electroceram.*, 2001, vol. 6, no. 1, pp. 61–74.
13. Hotta, Y., Tsunekawa, K., Isobe, T., Sato, K., and Watari, K., Synthesis of $BaTiO_3$ powders by a ball milling-assisted hydrothermal reaction, *Mater. Sci. Eng., Ser. A*, 2008, vol. 475, nos. 1–2, pp. 12–16.
14. Wei, X., Xu, G., Ren, Z., Wang, Y., Shen, G., and Han, G., Size-controlled synthesis of $BaTiO_3$ nanocrystals via a hydrothermal route, *Mater. Lett.*, 2008, vol. 62, no. 21, pp. 3666–3669.

15. McCormick, M.A. and Slamovich, E.B., Microstructure development and dielectric properties of hydrothermal $BaTiO_3$ thin films, *J. Eur. Ceram. Soc.*, 2003, vol. 23, no. 12, pp. 2143–2152.
16. Yuan, Y., Zhang, S.R., Zhou, X.H., and Tang, B., Effects of Nb_2O_5 doping on the microstructure and the dielectric temperature characteristics of barium titanate ceramics, *J. Mater. Sci.*, 2009, vol. 44, pp. 3751–3757.
17. Liu, L., Guo, H., Lü, H., Dai, Sh., Cheng, B., and Chen, Zh., Effects of donor concentration on the electrical properties of Nb-doped $BaTiO_3$ thin films, *J. Appl. Phys.*, 2005, vol. 97, no. 5, p. 054102.
18. Brzozowski, E., Castro, M.S., Foschini, C.R., and Stojanovic, B., Secondary phases in Nb-doped $BaTiO_3$ ceramics, *Ceram. Int.*, 2002, vol. 28, no. 7, pp. 773–777.
19. Shao, Y., Maunders, C., Rossouw, D., Kolodiazhnyi, T., and Botton, G.A., Quantification of the Ti oxidation state in $BaTi_{1-x}Nb_xO_3$ compounds, *Ultramicroscopy*, 2010, vol. 110, pp. 1014–1019.
20. Noh, H.-J., Lee, S.-G., Nam, S.-P., and Lee, Y.-H., Effect of sintering temperature on structural and dielectric properties of $(Ba_{0.54}Sr_{0.36}Ca_{0.10})TiO_3$ thick films, *Trans. El. Electron. Mater.*, 2009, vol. 10, no. 2, pp. 49–52.
21. Chen, C., Wei, Y., Jiao, X., and Chen, D., Hydrothermal synthesis of $BaTiO_3$: crystal phase and the Ba^{2+} ions leaching behavior in aqueous medium, *Mater. Chem. Phys.*, 2008, vol. 110, pp. 186–191.
22. Xu, H. and Gao, L., Hydrothermal synthesis of high-purity $BaTiO_3$ powders: control of powder phase and size, sintering density, and dielectric properties, *Mater. Lett.*, 2004, vol. 58, pp. 1582–1586.
23. Sun, W., Li, C., Li, J., and Liu, W., Microwave-hydrothermal synthesis of tetragonal $BaTiO_3$ under various conditions, *Mater. Chem. Phys.*, 2006, vol. 97, pp. 481–487.
24. Liu, S.-F., Abothu, I.R., and Komarneni, S., Barium titanate ceramics prepared from conventional and microwave hydrothermal powders, *Mater. Lett.*, 1999, vol. 38, pp. 344–350.
25. Sun, W. and Li, J., Microwave-hydrothermal synthesis of tetragonal barium titanate, *Mater. Lett.*, 2006, vol. 60, pp. 1599–1602.
26. Khanfekr, A., Tamizifar, M., and Naghizadeh, R., Micro-wave-hydrothermal synthesis and characterization of high-purity Nb doped $BaTiO_3$ nanocrystals, *J. Nanostruct.,* 2014, vol. 4, no. 1, pp. 31–36.
27. Newalkar, B.L., Komarneni, S., and Katsuki, H., Microwave-hydrothermal synthesis and characterization of barium titanate powders, *Mater. Res. Bull.*, 2001, vol. 36, pp. 2347–2355.
28. Liu, L., Guo, H., Lü, H., Dai, S., Cheng, B., and Chen, Z., Effects of donor concentration on the electrical properties of Nb-doped $BaTiO_3$ thin films, *J. Appl. Phys.*, 2005, vol. 97, p. 054102.
29. Ávila, H.A., Ramajo, L.A., Reboredo, M.M., Castro, M.S., and Parra, R., Hydrothermal synthesis of $BaTiO_3$ from different Ti-precursors and microstructural and electrical properties of sintered samples with submicrometric grain size, *Ceram. Int.*, 2011, vol. 37, no. 7, pp. 2383–2390.
30. Min, B., Moon, S.-M., and Cho, N.-H., Structural and dielectric features of Nb-doped nano-sized $BaTiO_3$ powders prepared by hydro-thermal synthesis methods, *Curr. Appl. Phys.*, 2011, vol. 11, no. 3, pp. S193–S196.
31. Lazarević, Z., Romcević, N., Vijatović, M., Paunović, N., Romcević, M., Stojanović, B., and Dohcevic-Mitrović, Z., Characterization of barium titanate ceramic powders by Raman spectroscopy, *Proceedings of the Tenth Annual Conference of the Materials Research Society of Serbia, YUCOMAT 2008, Herceg Novi, Montenegro, 2008, Acta Phys. Polonica, Ser. A,* 2009, vol. 115, no. 4, pp. 808–810.
32. Hai-Zhong, G., Li-Feng, L., Hui-Bin, L., and Yi-Yan, F., Structure, electrical, and optical properties of Nb-doped $BaTiO_3$ thin films grown by laser molecular beam epitaxy, *Chin. Phys. Lett.*, 2004, vol. 21, no. 2, pp. 396–399.
33. Jhung, S.H., Lee, J.H., Yoon, J.W., Hwang, Y.K., Hwang, J.S., Park, S.E., and Chang, J.S., Effects of reaction conditions in microwave synthesis of nanocrystalline barium titanate, *Mater. Lett.*, 2004, vol. 58, no. 25, pp. 3161–3165.
34. Hotta, Y., Tsunekawa, K., Duran, C., Sato, K., Nagaoka, T., and Watari, K., Low-temperature sintering of $BaTiO_3$ powders prepared by a hydrothermal process with ball milling system, *Mater. Sci. Eng., Ser. A*, 2008, vol. 475, pp. 57–61.
35. Newalkar, B.L., Komarneni, S., and Katsuki, H., Microwave-hydrothermal synthesis and characterization of barium titanate powders, *Mater. Res. Bull.*, 2001, vol. 36, no. 13–14, pp. 2347–2355.
36. Menéndez, J.A., Arenillas, A., Fidalgo, B., Fernández, Y., Zubizarreta, L., Calvo, E.G., and Bermúdez, J.M., Microwave heating processes involving carbon materials, *Fuel Process. Technol.*, 2010, vol. 91, no. 1, pp. 1–8.